PHYSICAL REVIEW E **76**, 030102(R) (2007)

Péclet-dependent memory kernels for transport in heterogeneous media

Andrea Cortis*
Earth Sciences Division, Lawrence Berkeley National Laboratory, Berkeley, California 94720, USA
(Received 30 May 2007; published 13 September 2007)

Transport in heterogeneous media can be described by partial differential equations, which exhibit convolutions with time and/or space memory kernels. In this work, we characterize the full time spectrum of time-memory kernels by applying a nonparametric inversion algorithm to macroscopic synthetic data for heterogeneous porous media, Our findings put into evidence the inherent nonuniqueness of the transport parameters for nonlocal transport models. Notably, we find that the Péclet number can be interpreted as an ancillary parameter of a family of probability distribution functions that characterizes the memory kernels of transport.

DOI: 10.1103/PhysRevE.76.030102 PACS number(s): 05.60.−k, 05.40.Fb

Transport of mass, momentum, and energy in multiscale heterogeneous systems is characterized, at a small scale, by the collective behavior of a large number of degrees of freedom that can be effectively described, at a mesoscopic scale, by advection and diffusion models. Transport in complex heterogeneous media differs from transport in homogeneous media mainly for its distinctively long first arrival times tails. An appropriate description of these long tails involves the convolution of the transport operators for homogeneous media with an appropriate (space and/or time) memory kernel. Transport in both aging [1–3] and nonaging [4] systems is fully characterized by time-memory kernels (nonlocality in time).

First principle derivations and direct measurements of time memory kernels remain open scientific challenges. For this reason, time memory kernels are often defined by low-dimensional parametrizations of simple analytical expressions. Such an approach, however, does not have enough flexibility to describe the distinctive features of more complex physical situations (e.g., multimodal arrival times and log-periodic fluctuations) and more flexible methods for extracting these kernels directly from macroscopic experimental observations are therefore needed.

The aim of this paper is twofold. First, we illustrate a numerical method aimed at the nonparametric inversion of the full time spectrum of the time-memory kernels. Second, we discuss some consequences of the results of this inversion method on the interpretation of the inverted parameters.

Many different formulations of transport in heterogeneous media, including the classical advection dispersion equation (ADE), fractional derivative equations (FDE), and multirate mass transfer (MRMT), can be shown to be special cases of the continuous time random walk (CTRW) formulation [4]. For this reason, and without loss of generality, in this work we develop the nonlocal equations of transport in the CTRW framework. In the CTRW framework, the master equation (ME) (mass balance) for the quantity of interest, say the concentration $c(x,\tau)$, reads

$$\partial_\tau c(x,\tau) = \int_\Omega w(x'-x)c(x',\tau)dx', \tag{1}$$

where τ is the (nondimensional) time, $w(x)$ is a transition rate, and x,x' are (nondimensional) spatial positions on a domain Ω. Equation (1) assumes a perfect knowledge of the transition rates $w(x'-x)$, and can be shown to yield the classical ADE description of transport [5]. These transition rates are, however, generally unknown (unresolved) in many physical situations and can be characterized only in a stochastic sense.

The key idea behind the CTRW approach is to map the unresolved structure of the small scale spatial heterogeneities onto a probability distribution function (PDF) of waiting times, $\Psi(x,\tau)$, which forms the core of the memory kernel. For this reason, Eq. (1) is ensemble averaged over all possible realizations of the unresolved heterogeneity to obtain the generalized master equation [6,7]

$$u\tilde{c}(x,u) - c_0(x) = \int_\Omega u\frac{\tilde{\Psi}(x'-x,u)}{1-\tilde{\psi}(u)}\tilde{c}(x',u)dx', \tag{2}$$

where the tilde indicates the Laplace transform (LT) $\tilde{f}(u) \equiv \mathcal{L}[f(\tau)] \equiv \int_0^\infty f(\tau)\exp(-u\tau)d\tau$, and u is the Laplace variable. The quantity $\tilde{\psi}(u) \equiv \int_0^\infty \tilde{\Psi}(x,u)dx$ is the conditional waiting time PDF and is the crucial quantity that we want to estimate from macroscopic experiments. Assuming that (i) the spatial and temporal components of $\tilde{\Psi}$ can be decoupled as $\tilde{\Psi}(x,u)=p(x)\tilde{\psi}(u)$ and that (ii) $p(x)$ (the PDF of the length of the jumps) has finite moments up to the second order, it is possible to define a local scale dispersivity α

$$\alpha \equiv \frac{1}{2}\frac{\int_\Omega p(x)x^2dx}{\int_\Omega p(x)xdx}, \tag{3}$$

which can be interpreted as the reciprocal of the Péclet number $\mathrm{Pe}=\alpha^{-1}$ when lengths are normalized with the first moment of $p(x)$.

*acortis@lbl.gov

A Taylor series expansion in x of the integrand on the right-hand side (RHS) of Eq. (2) yields the CTRW partial differential equation (PDE)

$$u\tilde{c}(x,u) - c_0(x) = \tilde{M}(u)\tilde{L}[c(x,u)], \tag{4a}$$

$$L[c(x,\tau)] = -\partial_x c(x,\tau) + \alpha\partial_{xx}c(x,\tau), \tag{4b}$$

where $c_0(x)$ is the initial condition, $\tilde{L}[\cdots]$ is the LT of the classical local-in-space linear transport operator, and $\tilde{M}(u) \equiv u\tilde{\psi}(u)/[1-\tilde{\psi}(u)]$ is a memory function that takes into account the nature of the heterogeneity. To solve Eq. (4) one needs to specify the nature of the heterogeneity by defining $\psi(\tau)$. The role of $\psi(\tau)$ is to map the structure of the unresolved heterogeneities onto a distribution of waiting times. Note that the special cases of $\tilde{\psi}=(1+u)^{-1}$ and $\tilde{\psi}=(1+u^{\beta})^{-1}$ (with $0<\beta<1$) correspond to the classical homogeneous transport, i.e., $\tilde{M}(u)=1$ and to the fractional in time derivative PDE of order β, respectively [4]. $\tilde{M}(u)$ may take various functional forms with respect to $\tilde{\psi}(u)$ for the case of colloidal transport in porous media [8] and aging systems [3].

Assuming Robin and Neumann boundary conditions (BCs) at the inlet and the outlet, respectively, the 1D Green function for Eq. (4) is

$$\tilde{c}(x,u) = \frac{(\zeta-1)e^{(x/2\alpha)(1+\zeta)} + (\zeta+1)e^{(x/2\alpha)}\left[\left(\frac{2}{x}-1\right)\zeta+1\right]}{[(\zeta+1)\xi+\alpha]e^{(1/\alpha)\zeta} + [(\zeta-1)\xi-\alpha]}, \tag{5}$$

where $\zeta=\sqrt{1+4\alpha\xi}$ and $\xi=(1-\tilde{\psi})/\tilde{\psi}$. The concentration $c(x,\tau)\equiv\mathcal{L}^{-1}[\tilde{c}(x,u)]$ can be obtained by solving the Fourier-Mellin integral line integral $c(x,\tau)=\int_{\gamma-i\infty}^{\gamma+i\infty}\tilde{c}(x,u)\exp(u\tau)du$. No analytical solution of $\mathcal{L}^{-1}$ for Eq. (5) is currently known, hence the original is evaluated numerically [9]. In this work, we use the inversion algorithm of de Hoog *et al.* [10], which makes use of complex-valued Laplace parameters u.

Direct observation of the $\psi(\tau)$ at the microscopic scale represents a formidable experimental challenge; moreover only a few first principles theoretical derivations exist [11–13]. In the context of transport in geological media, simple analytical models for $\psi(\tau)$ have been postulated based on asymptotic transport considerations [4,14]. In addition to the well studied power-law-like forms [15], another example of such a PDF is [12]

$$\psi(\tau) = \eta_3 F_3\left[\begin{matrix}1,1,1\\2,2,2\end{matrix}\;;\;-\tau\right]e^{-\eta\tau}{}_4F_4\left[\begin{matrix}1,1,1,1\\2,2,2,2\end{matrix}\;;\;-\tau\right], \tag{6}$$

where $\eta>0$ and ${}_pF_q$ is the generalized hypergeometric function

$${}_pF_q\left[\begin{matrix}a_1,\ldots,a_p\\b_1,\ldots,b_q\end{matrix}\;;\;x\right] = \sum_{k=0}^{\infty}\frac{\prod_{i=1}^{p}\Gamma(a_i+k)/\Gamma(a_i)}{\prod_{j=1}^{q}\Gamma(b_j+k)/\Gamma(b_j)}\frac{x^k}{k!}. \tag{7}$$

Regardless of the specific form of $L(x,\tau)$ in Eq. (4), the identification of the system parameters is obtained via a best fit procedure on the transport parameters of L (e.g., α) augmented with the parameters of the $\psi(\tau)$ (e.g., η). Such a parametric inversion can be easily implemented by means of a least-squares optimization on the experimental data [16]. If the solution of Eq. (4) does not fit the data adequately, a different functional form for $\psi(\tau)$ is postulated until a satisfactory fit is obtained. This is a very fortunate situation that is, however, not representative of the full spectrum of experimental data observed in many physical applications. Systems that exhibit a discrete spectrum of characteristic times, for instance, do not obey simple parametrizations of $\psi(\tau)$, and more general representations are needed. General expressions for $\psi(\tau)$, such as the one that represents the equivalence between CTRW and the MRMT [17–19]

$$\tilde{\psi}(u) \equiv \left(1 + u + u\sum_{i}^{N}\frac{\omega_i^{(t)}}{u+\omega_i^{(r)}}\right)^{-1} \tag{8}$$

become impractical as the number of parameters (the rates $\omega^{(r)}$ and $\omega^{(t)}$ in Eq. (8)) grows as $2N$, with N (the number of immobile phases) generally unknown. It is thus evident the need for a nonparametric inversion algorithm (NPIA) for ex-

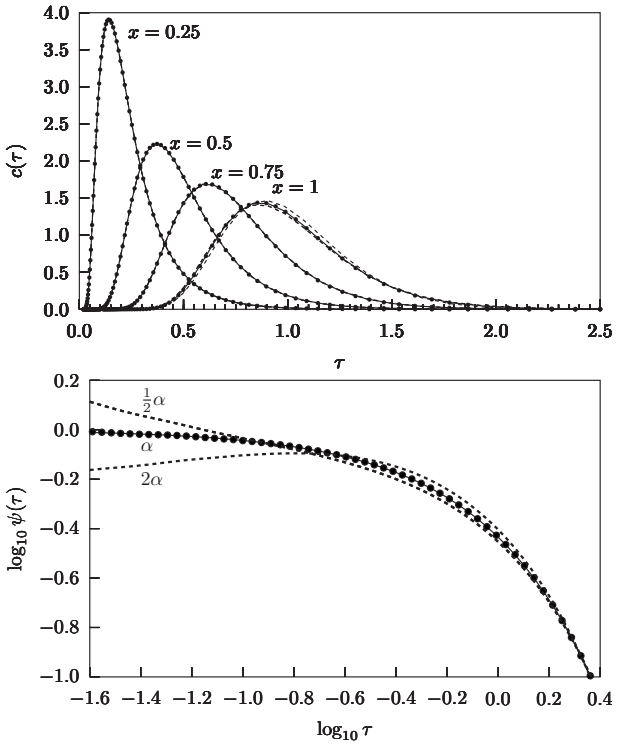

FIG. 1. Numerical solution of Eq. (5) for $\psi(\tau)=\exp(-\tau)$ and $\alpha=0.05$ (top: circles). The BTC at $x=0.25$ is taken as a baseline for the inversion and the inverted $\psi(\tau|\alpha=0.05)$ (bottom: circles) is compared to the original $\psi(\tau)$ (bottom: solid line). The predicted BTCs at $x=0.5$, 0.75, and 1.0 are calculated (top: solid line) and compared to the original numerical solution (top: circles). A perturbation to the value of α is applied and the corresponding $\psi(\tau|2\alpha)$ and $\psi(\tau|\frac{1}{2}\alpha)$ are calculated (bottom: dashed lines). The BTCs corresponding to these two perturbed $\psi(\tau)$ are calculated (top: dashed lines) and compared to the original analytical solutions.

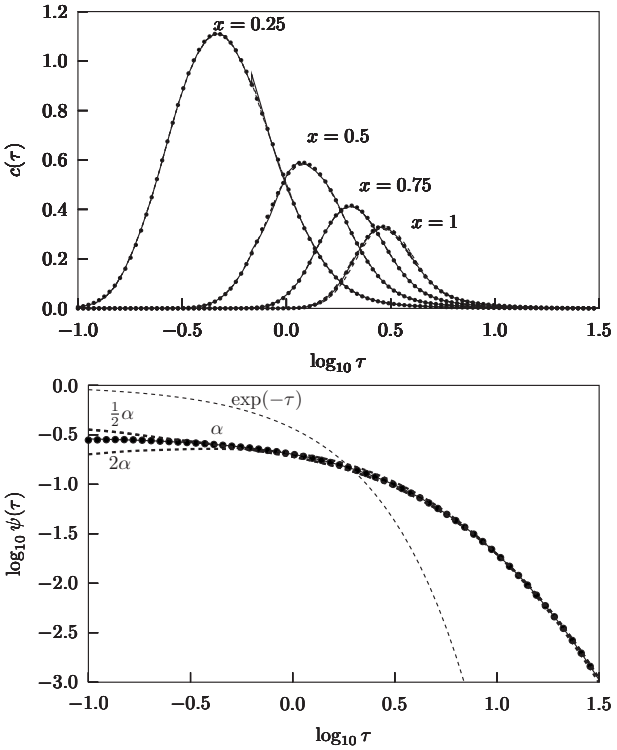

FIG. 2. Same as in Fig. 1, but with $\psi(\tau)$ described by Eq. (6) and a value of the disorder parameter $\eta=0.3$. The exponential decay $\exp(-\tau)$ is plotted for reference.

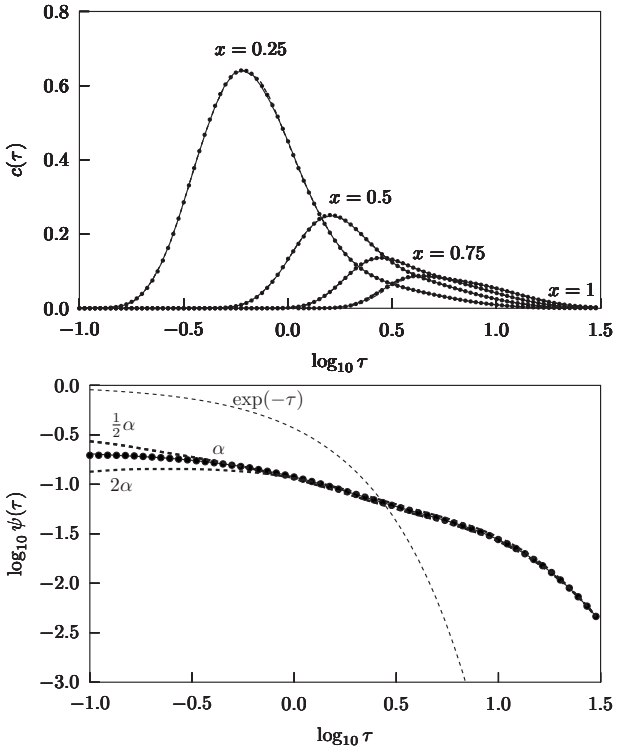

FIG. 3. Same as in Fig. 1, but with $\psi(\tau)=\Sigma_{k=1}^{3}a_k\exp(-b_k\tau)$, $a_k=[10,5,0.1]$, and $b_k=[1,0.1,0.01]$. The exponential decay $\exp(-\tau)$ is plotted for reference.

tracting the time-memory kernel $\tilde{M}(u)$ directly from experimental observations.

The aim of the NPIA is thus to find a numerical approximation for $\tilde{\psi}(u)$, by repeatedly minimizing the distance of the analytical solution (5) to the numerical LT of the experimental concentration $c_e(t)$ at each of the Laplace variables u_j. We assume an experimental breakthrough curve (BTC), $c_e(\tau)$ sampled at M times, $\tau_j\in[\tau_{\min},\tau_{\max}]$ at the section x. The $\hat{\mathcal{L}}^{-1}$ operator is defined by a complex valued sequence u_i with $i=1,\ldots,N$, such that $c(\tau_j)\equiv\mathcal{L}^{-1}[\tilde{c}(u_i)]$ (where we dropped the x dependence). We then evaluate a numerical approximation of $\mathcal{L}[c_e(\tau)]$ by truncating the LT to the experimental time interval

$$\int_0^{\infty} c_e(\tau)e^{-u_i\tau}d\tau \simeq \int_{\tau_{\min}}^{\tau_{\max}} c_e(\tau)e^{-u_i\tau}d\tau, \tag{9}$$

and calculating the integral on the right-hand side of Eq. (9) by means of a Clenshaw-Curtis quadrature algorithm.

It is important to stress that no *a priori* information on the value of α is generally available for a given transport experiment. We thus assume in Eq. (5) a value of α proportional to the nondimensional pore-scale characteristic length. We can now search for the value of $\tilde{\psi}_j|_\alpha$ introduced in Eq. (5) that minimizes the norm $\epsilon=||\tilde{c}_e(u_j)-\tilde{c}(u_j)||$, conditional to the value of α. This is done by a two-variables minimization of the real and imaginary parts of $\tilde{\psi}(u_j)$. A global minimum solution is enforced through a differential evolution search [20] followed by a Nelder-Mead unconstrained nonlinear minimization (e.g., $\epsilon<10^{-8}$). The minimization procedure is repeated for all the values of u_i to obtain an approximation of $\tilde{\psi}(u)$ that is used in Eq. (5) to evaluate $c(\tau_j)$ [9]. This numerical solution is then compared to the data $c_e(\tau_j)$. Finally, the waiting time distribution is inverted to obtain $\bar{\psi}(\tau)$, the numerical approximation of $\psi(\tau)$ in the $[\tau_{\min},\tau_{\max}]$ time interval.

To validate the inversion procedure, we consider three synthetic examples. The first example is the simple case of a PDF with an exponential decay $\psi(\tau)=\exp(-\tau)$, which corresponds to the classical transport in homogeneous media, i.e., $\tilde{M}(u)=1$. From Eq. (4), we calculated the BTCs at four spatial locations, $x=0.25,0.5,0.75,1$, for a value of $\alpha=0.05$. These four BTCs are shown as circles in 1 (top), and will be hereafter referred to as data. To initialize the NPIA, we select one of the four BTCs, in this case the BTC at $x=0.25$ and, keeping the value of $\alpha=0.05$ unchanged, we apply the NPIA described above to obtain the numerical approximation of the waiting time PDF $\bar{\psi}(\tau|\alpha)$, conditional on the chosen value of α. Both the original $\psi(t)=\exp(-\tau)$ and its numerical approximation $\bar{\psi}(\tau|\alpha)$ are plotted in Fig. 1 (bottom) as a solid line and circles, respectively. The $\bar{\psi}(\tau|\alpha)$is then used to evaluate the BTC at sections $x=0.5,0.75,1$. These BTCs are plotted in Fig. 1 (top) as solid lines and show excellent agreement with the data. From these results, we can conclude that the numerical approximation of $\psi(\tau)$ in the interval definition for the BTC does provide enough information to re-

produce the whole behavior of the system. This result is, however, not very surprising as we set α to the value used in the data generation. In the more general case of experimental BTCs, though, we do not have access to this information and we need to assume a reasonable value for the dispersivity α.

To check the sensitivity of the NPIA to variations of the value of α, we repeated the procedure perturbing α by the factors 0.5 and 2, respectively. The resulting BTCs are shown in Fig. 1 (dashed lines) and are indistinguishable from the data (solid lines) at $x=0.25,0.5,0.75$. Some minor deviations can be observed for $x=1$, attributable to numerical approximations. The shapes of the corresponding waiting time pdfs, as expected, exhibit significative deviations from the originally imposed exponential decay $\psi(\tau)=\exp(-\tau)$ (see Fig. 1 bottom, dashed lines). These findings imply the existence of an overlap between the local in space dispersivity α, and the nonlocal in time waiting time PDF $\psi(\tau|\alpha)$ descriptions of the BTC apparent dispersion. This overlap entails an inherent nonuniqueness of the inverted transport parameters, coherently with nonlocal descriptions of transport such as the CTRW.

The second example involves data generated by means of the long tailed waiting time PDF in Eq. (6) for a value of $\eta=0.3$. Figure 2 (bottom) shows this $\psi(\tau)$ as circles (the exponential decay is reported for reference as a dashed line). The results for this test case are qualitatively analogous to the ones obtained in the first example.

The third example (see Fig. 3), involves a waiting time distribution of the form $\psi(t)=\Sigma_{k=1}^{3}a_k\exp(-b_k\tau)$, with $a_k=[10,5,0.1]$ and $b_k=[1,0.1,0.01]$. Also in this case, we obtain an excellent match between the inverted results and the data.

In all the three test cases reported above, the baseline BTC was taken at $x=0.25$, and the other BTCs at $x=0.5,0.75$, and 1 were predicted. The agreement between the predicted BTCs and the data, however, is conserved upon a change in the baseline section, indicating that each of the four BTCs contains the necessary information to describe the whole spatiotemporal behavior of the heterogeneous system. The NPIA thus returns a one-parameter family of equivalent PDFs, $\bar{\psi}(\tau|\alpha)$, which model equally well the transport data. This nonuniqueness can be understood by recalling that, in nonlocal in time frameworks, the only requirement on $p(x)$, is one of finite first and second moments. The actual value of these two moments, however, is not specified so that their ratio α (hence the Péclet number) in Eq. (3) becomes an ancillary parameter of a more general characterization of transport, the waiting time PDF $\bar{\psi}(\tau|\alpha)$. Our NPIA can also be used to infer transport characteristics from spatial profiles and can be adapted to any nonlocal description of transport. The proposed NPIA inversion and the associated physical interpretation should prove useful in the characterization, understanding, and prediction of the rich complexity of transport phenomena in multiscale heterogeneous media.

We thank B. Faybishenko, D. Silin, J. Berryman, and two anonymous reviewers for useful discussions and comments. This work was supported, in part, by the U.S. Department of Energy under Contract No. DE-AC02-05CH11231.

[1] G. Margolin and E. Barkai, J. Chem. Phys. **121**, 1566 (2004).
[2] P. Allegrini, G. Aquino, P. Grigolini, L. Palatella, A. Rosa, and B. J. West, Phys. Rev. E **71**, 066109 (2005).
[3] P. Allegrini, F. Barbi, P. Grigolini, and P. Paradisi, Phys. Rev. E **73**, 046136 (2006).
[4] B. Berkowitz, A. Cortis, M. Dentz, and H. Scher, Rev. Geophys. **44**, 1 (2006).
[5] B. Berkowitz, J. Klafter, R. Metzler, and H. Scher, Water Resour. Res. **38**, 1191 (2002).
[6] V. M. Kenkre, E. W. Montroll, and M. F. Shlesinger, J. Stat. Phys. **9**, 45 (1973).
[7] J. Klafter and R. Silbey, Phys. Rev. Lett. **44**, 55 (1980).
[8] A. Cortis, T. Harter, L. Hou, E. R. Atwill, A. Packman, and P. Green, Water Resour. Res. **42**, W12S13 (2006).
[9] A. Cortis and B. Berkowitz, Ground Water **43**, 947 (2005).
[10] F. R. de Hoog, J. H. Knight, and A. N. Stokes, SIAM (Soc. Ind. Appl. Math.) J. Sci. Stat. Comput. **3**, 357 (1982).
[11] H. Scher and M. Lax, Phys. Rev. B **7**, 4491 (1973).
[12] A. Cortis, Y. Chen, H. Scher, and B. Berkowitz, Phys. Rev. E **70**, 041108 (2004).
[13] M. Dentz and B. Berkowitz, Phys. Rev. E **72**, 031110 (2005).
[14] B. Berkowitz and H. Scher, Phys. Rev. Lett. **79**, 4038 (1997).
[15] M. Dentz, A. Cortis, H. Scher, and B. Berkowitz, Adv. Water Resour. **27**, 155 (2004).
[16] A. Cortis and B. Berkowitz, Soil Sci. Soc. Am. J. **68**, 1539 (2004).
[17] J. Carrera, X. Sánchez-Vila, I. Benet, A. Medina, G. Galarza, and J. Guimerà, Hydrogeol. J. **6**, 178 (1998).
[18] R. Haggerty, S. A. McKenna, and L. C. Meigs, Water Resour. Res. **36**, 3467 (2000).
[19] M. Dentz and B. Berkowitz, Water Resour. Res. **39**, 1111 (2003).
[20] K. Price, R. Storn, and J. Lampinen, *Differential Evolution - A Practical Approach to Global Optimization* (Springer, Berlin, 2005).